Thermal Behavior and Phase Transformation of TiO$_2$ Nanocrystallites Prepared by a Coprecipitation Route

SHANG-WEI YEH, YEN-LING CHEN, CHI-SHIUNG HSI, HORNG-HUEY KO, and MOO-CHIN WANG

TiO$_2$ freeze-dried precursor powders were synthesized using a coprecipitation route that includes titanium tetrachloride (TiCl$_4$) as initial material prepared at 348 K (75 °C) and pH 7. Differential scanning calorimetry/thermogravimetry (DSC/TG), X-ray diffraction (XRD), transmission electron microscopy (TEM), and selected area electron diffraction (SAED) and high resolution TEM were utilized to characterize the thermal behavior and phase transformation of the TiO$_2$ freeze-dried precursor powders after calcination. The main compound of the TiO$_2$ freeze-dried precursor powders was TiO$_2$·H$_2$O based on a TG analysis conducted at a heating rate of 20 K (20 °C)/min. The anatase TiO$_2$ (a-TiO$_2$) first appeared at 473 K (200 °C), then from a-TiO$_2$ transformed to rutile TiO$_2$ (r-TiO$_2$) at 773 K (500 °C). The activation energy of a-TiO$_2$ formation from TiO$_2$ freeze-dried precursor powders was 242.4 ± 33.9 kJ/mol, whereas, the activation energy of phase transformation from a-TiO$_2$ to r-TiO$_2$ was 267.5 ± 19.1 kJ/mol. The crystallite size of a-TiO$_2$ grew from 3.5 to 23.2 nm when raising the calcination temperature from 473 K to 873 K (200 °C to 600 °C). In addition, the crystallite size of r-TiO$_2$ increased from 17.4 to 48.1 nm when calcination temperature increased from 773 K to 1073 K (500 °C to 800 °C).

I. INTRODUCTION

TiO$_2$ is one of the important inorganic material, widely used in sunscreen,[1] photocatalyst,[2,3] and sensors.[4,5] TiO$_2$ possesses three crystal structures: anatase, rutile, and brookite.[6] The anatase and rutile phases are Ti-O octahedral which formed a tetragonal structure, otherwise, the brookite phase formed an orthorhombic.[6] The common phases of TiO$_2$ are anatase and rutile, where the rutile is the most stable one among the three phases. The phase transformation from anatase and brookite to rutile occurred when the anatase and brookite were calcined between 623 K to 1478 K (350 °C to 1175 °C),[7] and 773 K to 873 K (500 °C to 600 °C),[8] respectively.

Recently, numerous techniques have been widely used for synthesizing the TiO$_2$ nanopowders that have greater control properties, such as the coprecipitation,[9,10] hydrothermal,[11,12] and sol–gel method.[13,14] Among these, homogeneous precipitation is one of the most promising techniques because of the advantages of low cost, easy-to-acquire equipments, a simple synthesis process, and nanometric precursor particles. Using the coprecipitation route for synthesis, the amorphous TiO$_2$ precursor powders were obtained for the precipitation through freeze-drying process. After calcinations, the crystalline TiO$_2$ powders were obtained. Hsiang et al.[15,16] have pointed out that the activation energies of a-TiO$_2$ and r-TiO$_2$ crystallization were obtained, namely, 53 to 250 kJ/mol and 205 to 506 kJ/mol, respectively, and the values were dependent on aging process. The value of activation energy for TiO$_2$ crystallization with aging treatment was higher than that without aging. In addition, Kumar et al.[17,18] also proposed that the activation energy of phase transformation from a-TiO$_2$ transformed to r-TiO$_2$ was 147 kJ/mol for the titania membranes prepared by sol–gel process. However, thermal behavior and phase transformation of TiO$_2$ freeze-dried precursor powders prepared by a coprecipitation route have not been discussed in detail.

In the present study, the TiO$_2$ freeze-dried precursor powders synthesized using titanium tetrachloride as initial material prepared by a coprecipitation route were investigated. The thermal behavior and phase transformation of TiO$_2$ freeze-dried precursor powders after calcination were investigated using differential scanning calorimetry/thermogravimetry (DSC/TG), X-ray diffractometer (XRD), transmission electron microscopy (TEM), selected area electron diffraction (SAED), and high resolution TEM (HRTEM). The purposes of the present work include: (1) study the thermal behavior of TiO$_2$ freeze-dried precursor powders, (2) investigate the phase transformation of the TiO$_2$ freeze-dried precursor powders after calcination, (3) study the crystallite growth behavior of a-TiO$_2$ and r-TiO$_2$, and (4) observe the microstructure of calcined TiO$_2$ powders.

SHANG-WEI YEH, Graduate Student, YEN-LING CHEN, Assistant Professor, HORNG-HUEY KO, Associate Professor, and MOO-CHIN WANG, Professor, are with the Department of Fragrance and Cosmetic Science, Kaohsiung Medical University, 100 Shih-Chuan 1st Road, Kaohsiung 80782 Taiwan R.O.C. Contact e-mail: mcwang@kmu.edu.tw CHI-SHIUNG HSI, Professor, is with the Department of Materials Science and Engineering, National United University, 1 Lein-Da, Kung-Ching Li, Miao-Li 36003, Taiwan R.O.C.
Manuscript submitted March 14, 2013.
Article published online August 30, 2013.

II. EXPERIMENTAL PROCEDURE

A. Sample Preparation

Titanium tetrachloride (TiCl$_4$, purity ~98.5 pct, supplied by Nihon Shiyaku Reagent, Japan) was used as starting material for a coprecipitation process. TiCl$_4$ was dissolved in deionized water with a volume ratio of 1:20, and the mixed solution was stirred using a magnetic stirrer and heated to 348 K (75 °C) for 2 hours, then Ti^{4+} solution was formed. Since the pH value of Ti^{4+} solution was very low and no precipitation occurred. In order to increase the pH value for accelerating the precipitation, the mixed solution must be added with the precipitation agent. In the present study, the NH$_4$OH aqueous solution was used as the precipitation agent. When the NH$_4$OH aqueous solution (purity ~28 pct, supplied by Nihon Shiyaku Reagent, Japan) was added to water-TiCl$_4$ mixture, [OH$^-$] concentration increased resulting the pH value increase. This result can be expressed as following reaction:

$$Ti^{4+} + 4OH \rightarrow TiO(OH)_2 + H_2O \qquad [1]$$

Moreover, when the pH value of water-TiCl$_4$ mixed solution was adjusted to 0.5, the precipitation reaction reoccurred. The OH$^-$ ions will promote the interparticle repulsion to enhance the dispersiveness and caused the particle size decrease. Therefore, the pH value of present study was adjusted to 7.

After precipitation, the precipitates were washed with a large amount of deionized water for five times. Subsequently, the precipitates were freeze-dried at 218 K (−55 °C) in vacuum.

B. Sample Characterization

Differential scanning calorimetry/thermogravimetry (DSC/TG) (SDT Q600, TA) analysis was conducted on a 200 mg freeze-dried precursor powders sample at various rates in static air up to 1173 K (900 °C). Al$_2$O$_3$ powders were used as the reference material.

The crystalline phases of the TiO$_2$ freeze-dried precursor powders after calcination were identified by X-ray diffraction (XRD, Model Rad IIA, Rigaku, Tokyo) with Cu K$_\alpha$ radiation and an Ni filter, operating at 40 kV, 30 mA and a scanning rate (2θ) of 1 deg/min.

When the TiO$_2$ freeze-dried precursor powders were calcined at various temperatures for 120 minutes, the morphology of calcined TiO$_2$ freeze-dried precursor powders was examined using TEM (JEM 2100F, JEOL, Japan) at an operating voltage 200 kV. The TEM sample was prepared by dispersing the calcined powders in an ultrasonic bath and then collecting them on a copper grid. The TiO$_2$ crystalline structure was determined by SAED based on TEM.

III. RESULTS AND DISCUSSION

A. Thermal Behavior of TiO$_2$ Freeze-Dried Precursor Powders

The DSC/TG curves of the TiO$_2$ freeze-dried precursor powders heated in static air at a rate of 10 K/min (10 °C/min) from 303 K to 1173 K (30 °C to 900 °C) were shown in Figure 1. The TG curve shows that the mass loss of TiO$_2$ freeze-dried precursor powders took place in a wide temperature range from room temperature to 873 K (600 °C), which indicate that the mass loss was almost present at an exponential decay from 373 K to 723 K (100 °C to 450 °C). The TG curve of TiO$_2$ freeze-dried precursor powders can be divided to three loss stages: (i) from room temperature to 373 K (100 °C), (ii) from 373 K to 723 K (100 °C to 450 °C) as the main mass loss, and (iii) from 723 K to 873 K (450 °C to 600 °C), when heating temperature was higher than 873 K (600 °C), the mass was maintained nearly stable.

In Figure 1, the first mass loss of about 5.7 pct was attributed to the free water of physisorbed water.[19] In the second stage, about 17.9 pct of mass loss occurred. This result can be expressed as following reaction:

$$TiO(OH)_2 \rightarrow TiO_2 + H_2O \qquad [2]$$
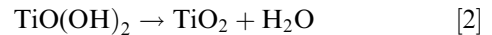
The third mass loss of about 1.2 pct can be assigned to the further hydration of the surface water molecules most likely existing in a wide set of energetically non-equivalent surface hydrogen groups.[20]

Nakayama[21] has pointed out that when water molecule and hydroxyl ions decomposed from TiO$_2$·xH$_2$O, residual 82 wt pct of TiO$_2$ was the product. In this study, the residual TiO$_2$ of freeze-dried precursor powders residual was about 77.6 wt pct, which revealed that TiO$_2$·H$_2$O was the main compound in the freeze-dried precursor powders.

In this study, hydrolysis of the titanium cation occurred at a low pH level. The first hydrolysis step caused the formation of [Ti(OH)(OH$_2$)$_5$]$^{3+}$ species, which were stable under strong acid conditions. These species were not able to condense due to the positive change of the hydroxo group.[22] Condensation to both anatase and rutile began when the solution activity was high enough to allow further deprotonation to [Ti(OH)$_3$(OH$_2$)$_3$]$^+$, depending on the exact pH.[22] At a high pH level, when deoxolation occurred, condensation
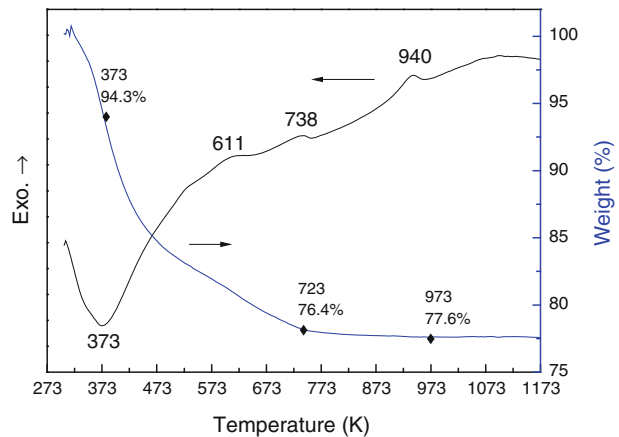

Fig. 1—The DSC/TG curves for TiO$_2$ freeze-dried precursor powders heated at a rate of 10 K/min (10 °C/min) from 303 K to 1173 K (30 °C to 900 °C) in a static air.

can proceed along apical direction created the skewed chains of the anatase structure.[23,24]

In addition, the DSC curve also showed that one endothermic peak at 373 K (100 °C), and three exothermic peaks at 611 K, 738 K, and 940 K (338 °C, 465 °C, and 667 °C). The one endothermic peak at 373 K (100 °C) was attributed to the dehydration from the surface of precursor powders.[25] Moreover, the first broad exothermic peak at 611 K (338 °C) due to the hydroxyl groups was eliminated and the Ti-O-Ti bonds were formed.[20] Above results caused the endothermic reaction but the peak at 611 K (338 °C) had a broad exothermic peak, which was due to the anatase TiO_2 (a-TiO_2) formed. The second exothermic peak at 738 K (465 °C) was attributed to the phase transformation from a-TiO_2 to rutile TiO_2 (r-TiO_2). Furthermore, the final exothermic peak at 940 K (667 °C) was caused by the a-TiO_2 fully converted to r-TiO_2.

B. *The Phase Transformation of the TiO_2 Freeze-Dried Precursor Powders After Calcinations at Various Temperatures for 120 Minutes*

Figure 2 shows the XRD patterns of the TiO_2 freeze-dried precursor powders after calcination at various temperatures for 120 minutes. The XRD pattern of the TiO_2 freeze-dried precursor powders was shown in Figure 2(a), which revealed that the precursor powders before calcinations maintained its amorphous state. Figure 2(b) shows the XRD pattern of the TiO_2 freeze-dried precursor powders after calcination at 473 K (200 °C), it was seen that the (101), (004), and (200) reflection peaks of a-TiO_2 first appeared. The XRD pattern of the TiO_2 freeze-dried precursor powders after calcination at 573 K (300 °C) was shown in Figure 2(c), and indicated that the phase still maintained the a-TiO_2. However, the reflections shown in Figure 2(c) were still weak and broad due to poor crystallinity and a small crystallites in the submicron to nanometer range.[26,27] Figure 2(d) shows the XRD pattern of the TiO_2

Fig. 2—The XRD patterns of TiO_2 freeze-dried precursor powders after calcination at various temperatures for 120 min: (*a*) uncalcined, (*b*) 473 K (200 °C), (*c*) 573 K (300 °C), (*d*) 673 K (400 °C), (*e*) 773 K (500 °C), (*f*) 873 K (600 °C) and (*g*) 973 K (700 °C). *R* denoted the r-TiO_2, *A* denoted the a-TiO_2.

freeze-dried precursor powders after calcination at 673 K (400 °C), which revealed that the all reflection peaks still maintained the a-TiO_2 phase. But the intensity of (101) reflection of a-TiO_2 was greater than that of Figure 2(c) due to the enhanced crystallinity of a-TiO_2 when raising the calcination temperature from 573 K to 673 K (300 °C to 400 °C). The XRD pattern of TiO_2 freeze-dried precursor powders after calcination at 773 K (500 °C) for 120 minutes was shown in Figure 2(e). It was seen that all the reflection peaks still belonged to the a-TiO_2 phase, except the (110) reflection of r-TiO_2 first appeared but the intensity was very weak. Moreover, according to the Figures 2(b) through (e), it was also seen that the intensities of all reflection peaks of Figure 2(e) were higher than that of other patterns and the half width of full maximum (HWFM) intensity of a-TiO_2 (101) decreased. This result was due to the crystallinity and crystallite size of a-TiO_2 increased with raising the calcination temperatures. The XRD pattern of the TiO_2 freeze-dried precursor powders after calcination at 873 K (600 °C) for 120 minutes was shown in Figure 2(f), which indicated that the a-TiO_2 phase still maintained and the (110), (101), (111), and (211) reflections peaks of r-TiO_2 first appeared. Although the phases were a-TiO_2 and r-TiO_2 coexisting but the HWFM of a-TiO_2 (101) reflection decreased. In addition, the (110), (101), (111), and (211) reflections of r-TiO_2 were improved with raising the calcination temperatures. Figure 2(g) shows the XRD pattern of the TiO_2 freeze-dried precursor powders after calcination at 973 K (700 °C), which indicated that the a-TiO_2 phase was fully converted to r-TiO_2.

Using the intensity of the reflection (h k l) in the XRD pattern to determine the a-TiO_2 content has been proposed by Spurr and Myers.[28] The integrated intensity ratio of the a-TiO_2 content was defined by

$$f_A = \frac{1}{1 + 1.265 \frac{I_R}{I_A}}, \qquad [3]$$

where f_A was the fraction of the a-TiO_2, I_R and I_A were the intensities of the (101) and (110) reflections for a-TiO_2 and r-TiO_2, respectively.

Figure 3 shows the phase contents of a-TiO_2 and r-TiO_2 when the freeze-dried precursor powders after calcination between 473 K and 973 K (200 °C and 700 °C) for 120 minutes. The results of Figure 3 show that the a-TiO_2 was 100 pct when the TiO_2 freeze-dried precursor powders after calcination between 473 K and 673 K (200 °C and 400 °C) for 120 minutes. When the TiO_2 freeze-dried precursor powders were calcined at 773 K (500 °C) for 120 minutes, the phase contents of a-TiO_2 and r-TiO_2 were 88 and 12 pct, respectively. When raising the calcination temperature of the TiO_2 freeze-dried precursor powders from 773 K to 973 K (500 °C to 700 °C), the phase contents of a-TiO_2 decreased from 88 to 0 pct, whereas the r-TiO_2 content increased from 12 to 100 pct.

Using $TiCl_4$ and NH_4OH as the initial materials for preparing the TiO_2 precursor powders by a microemulsion process at room temperature has been reported by Keswani *et al.*[29] They proposed that the phase of
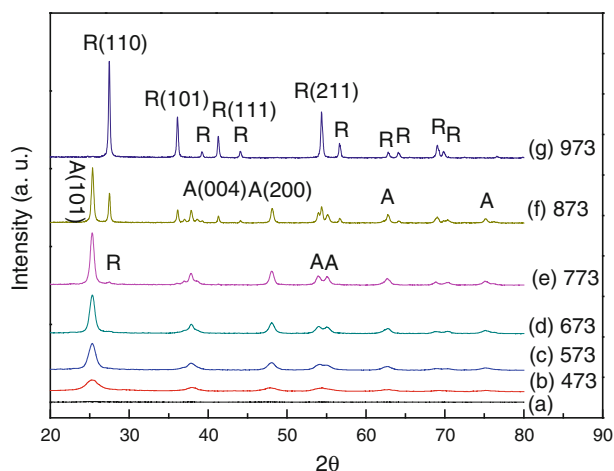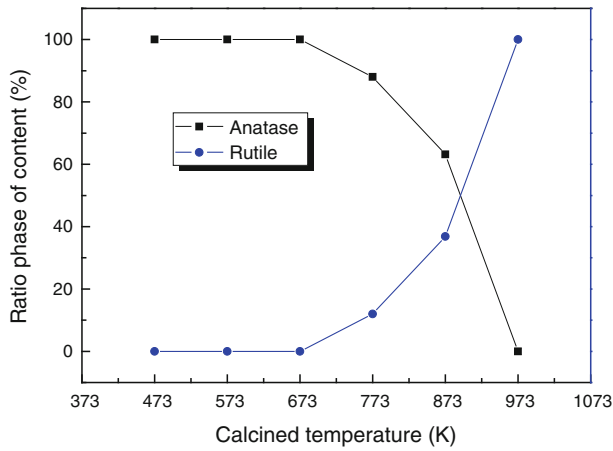
Fig. 3—The ratio of anatase and rutile phases of TiO$_2$ freeze-dried powders after calcination at various temperatures for 120 min.

Fig. 5—DSC curves of the TiO$_2$ freeze-dried precursor powders at various heating rates: (a) 5, (b) 10, (c) 15, and (d) 20 K/min (5, 10, 15, and 20 °C/min).
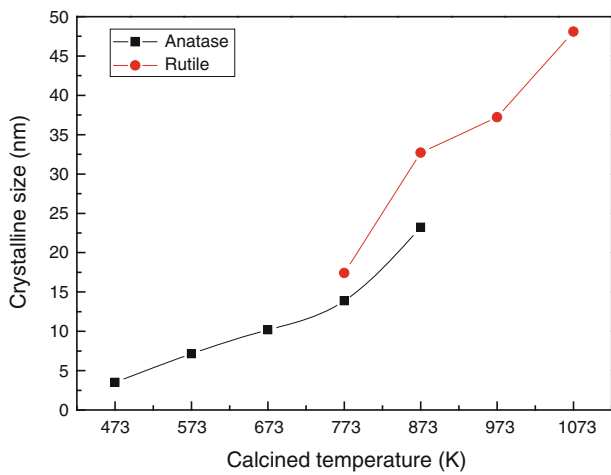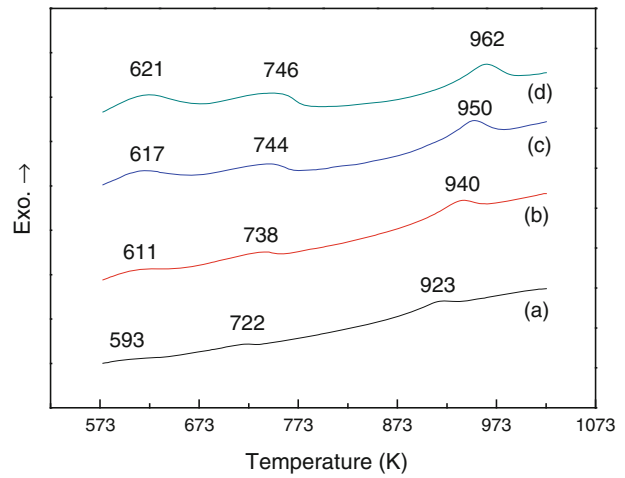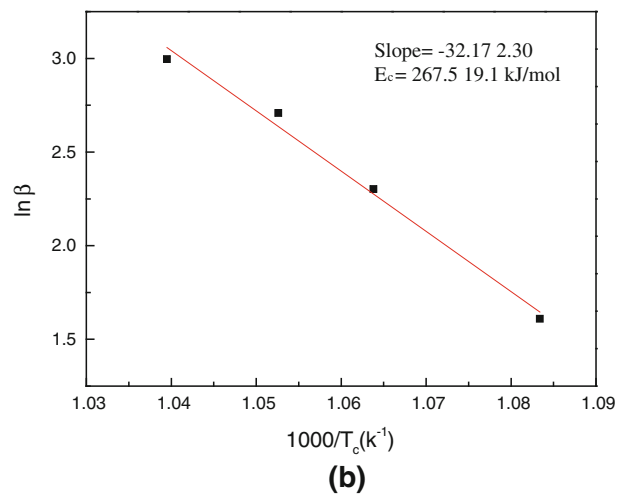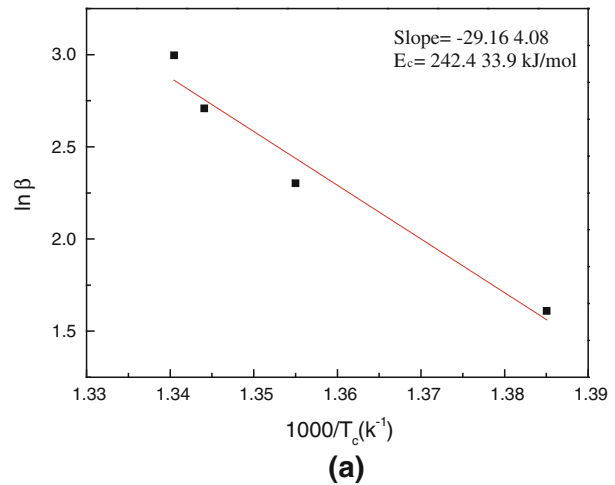

Fig. 4—Crystallite size of TiO$_2$ freeze-dried powders after calcination at various temperatures for 120 min.

a-TiO$_2$ still existed when calcined at 1173 K (900 °C) for 4 hours. This result did not agree with the ones of the present study. The difference between these investigations can be caused by the different synthesized method and temperature used. On the other hand, Marinescu et al.[30] also used the soluble salts of titanium and NH$_4$Cl as the initial materials by a hydrothermal process for preparing the TiO$_2$ precursor powders. They have pointed out that the anatase to rutile phase transformation depended not only on primary crystallite size but also on the presence of the brookite phase and absorbed water. The presence of the brookite phase accelerated the anatase to rutile transformation.[30] The difference of results between the present study, and the result of Marinescu et al.[30] could be due to the various preparing method.

C. The Crystallite Size of the TiO$_2$ Freeze-Dried Precursor Powders After Calcination

The crystallite size (D) of the a-TiO$_2$ and r-TiO$_2$ was calculated using Scherrer's equation:[31]

Fig. 6—Plots of ln β vs 1000/T_c for TiO$_2$ freeze-dried precursor powders after calcination at various heating rate (β): (a) a-TiO$_2$ and (b) r-TiO$_2$. E_c denoted the crystallization activation energy.

$$D = \frac{0.9\lambda}{\beta \cos \theta}, \qquad [4]$$

where $\lambda = 1.5405$ Å was the wavelength of Cu K_α radiation, β was the full-width at half-maximum (FWHM) intensity in radians. The $(101)_a$ and $(110)_r$ reflections at $2\theta = 25.32$ and 27.48 deg were used to define the FWHM intensity of anatase and rutile TiO_2, respectively, within various crystalline phases, and θ was the Bragg's angle.

The crystallite sizes of the TiO_2 freeze-dried precursor powders after calcination at various temperatures for 120 minutes were shown in Figure 4. It was seen that the average crystallite sizes of a-TiO_2 and r-TiO_2 powders increased with raising the calcination temperatures. Moreover, it was also seen that when duration for 120 minutes, the crystallite size of a-TiO_2 increased from 3.5 to 23.2 nm with raising the calcination temperature from 473 K to 873 K (200 °C to 600 °C). Moreover, the crystallite size of

r-TiO_2 increased from 17.4 to 48.1 nm with raising temperature from 773 K to 1073 K (500 °C to 800 °C).

The result of Figure 4 also revealed that the crystallite sizes of TiO_2 still maintained the nanosize range, when the freeze-dried precursor powders were calcined between 473 K and 1073 K (200 °C to 800 °C) for 120 minutes.

D. The Crystallization Behavior of TiO₂ Freeze-Dried Precursor Powders After Calcination

The DSC curves of the TiO_2 freeze-dried precursor powders at various heating rate in static air from 573 K to 1023 K (300 °C to 750 °C) were shown in Figure 5. It was seen that the crystallization temperatures of a-TiO_2 were between 593 K and 621 K (320 °C and 348 °C). The temperatures of phase transformation from a-TiO_2 to r-TiO_2 were between 722 K and 750 K (449 °C and 473 °C), and the final exothermic peak temperatures were between 932 K and 962 K (650 °C and 689 °C). In
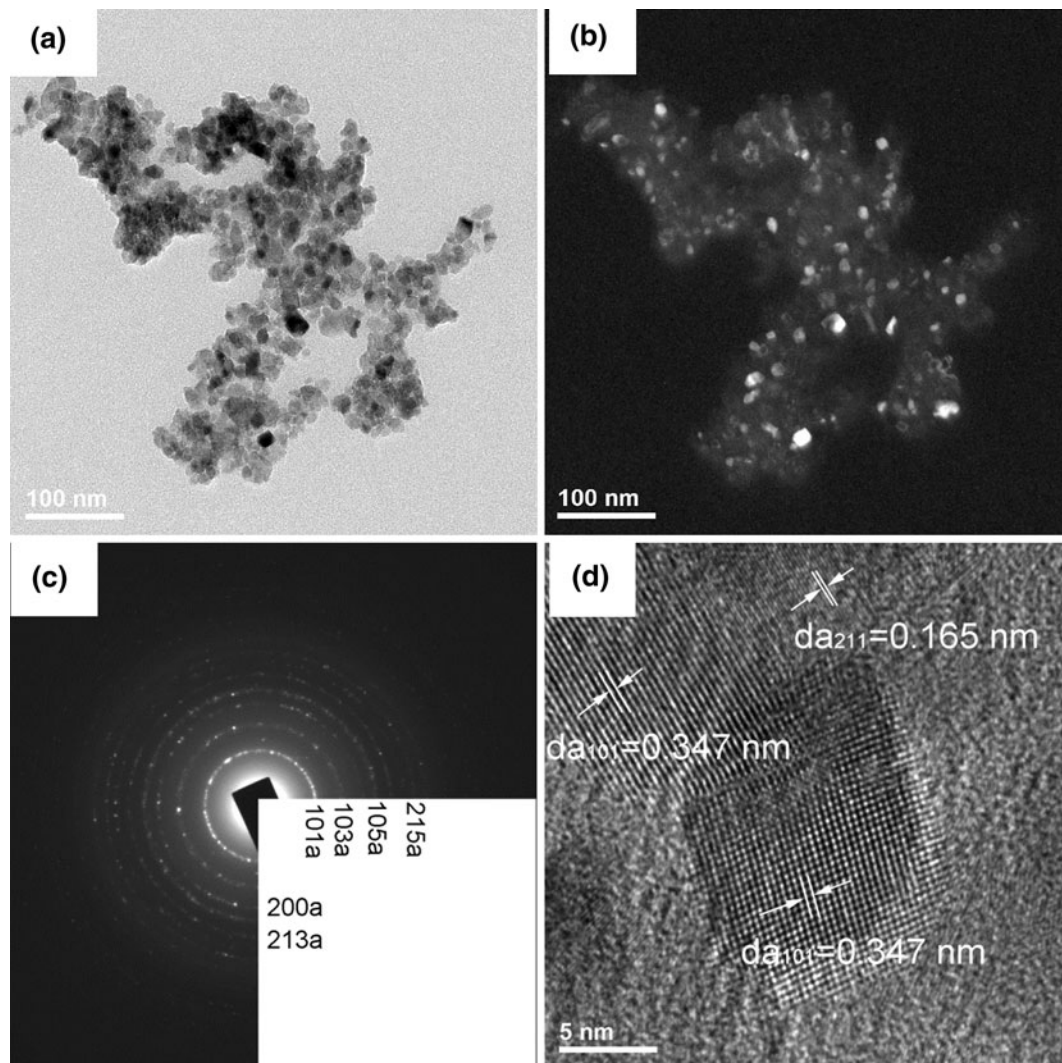

Fig. 7—TEM micrographs of TiO₂ freeze-dried precursor powders after calcination at 673 K (400 °C) for 120 minutes: (*a*) BF image, (*b*) DF image using a-TiO₂ (101) in (*c*), (c) SAED pattern which indexed corresponding to a-TiO₂, (d) HRTEM image with *d*-spacing of the a-TiO₂ (101) and (111) were 0.347 and 0.165 nm, respectively.

addition, Figure 5 also shows that the exothermic peaks shifted to higher temperatures with raising the heating rate. This phenomenon was attributed to the higher heating rates and resulting in the transition temperature leaving the equilibrium transition point and shifting to a higher temperature. In the present study, the exothermic peak temperatures of the DSC curves can be used to derive the activation energy of phases crystallization from the TiO_2 freeze-dried precursor powders using the Johnson–Mehl–Avrami (JMA) equation;[32]

$$\ln \beta = -\frac{E_c}{RT_c} + \ln CM, \qquad [5]$$

where β meant the heating rate (K/min), E_c denoted the crystallization activation energy (kJ/mol), R was the gas constant (8.314 J/mol), T_c was the absolute temperature (K) that corresponded to the exothermic peak of crystallization, and $\ln CM$ was a constant.

Figure 6 shows that the linear relationship between $\ln \beta$ and $1/T_c$ for various TiO_2 formations in freeze-dried precursor powders. The slopes of the fitting lines were -29.16 ± 4.08 and -32.17 ± 2.30 for a-TiO_2 and r-TiO_2, respectively. Therefore, the apparent activation energies of a-TiO_2 and r-TiO_2 formation in the precursor powders were calculated from the slopes to be 242.4 ± 33.9 kJ/mol and 267.5 ± 19.1 kJ/mol, respectively. The phases formed from the different raw materials and synthesis processes were directly dependent on the chemical homogeneity of the components.[33] The activation energy value of r-TiO_2 was in agreement with the value of r-TiO_2 formation from the precursor obtained by Ti^{4+} solution with NH_4OH coprecipitation at pH 9 and without aging treatment.[16]

Zhang and Banfield[34] have pointed out that the activation energy of the a-TiO_2 crystallization was 78 kJ/mol. Moreover, the activation energy of phase transformation from a-TiO_2 to r-TiO_2 was 147 kJ/mol
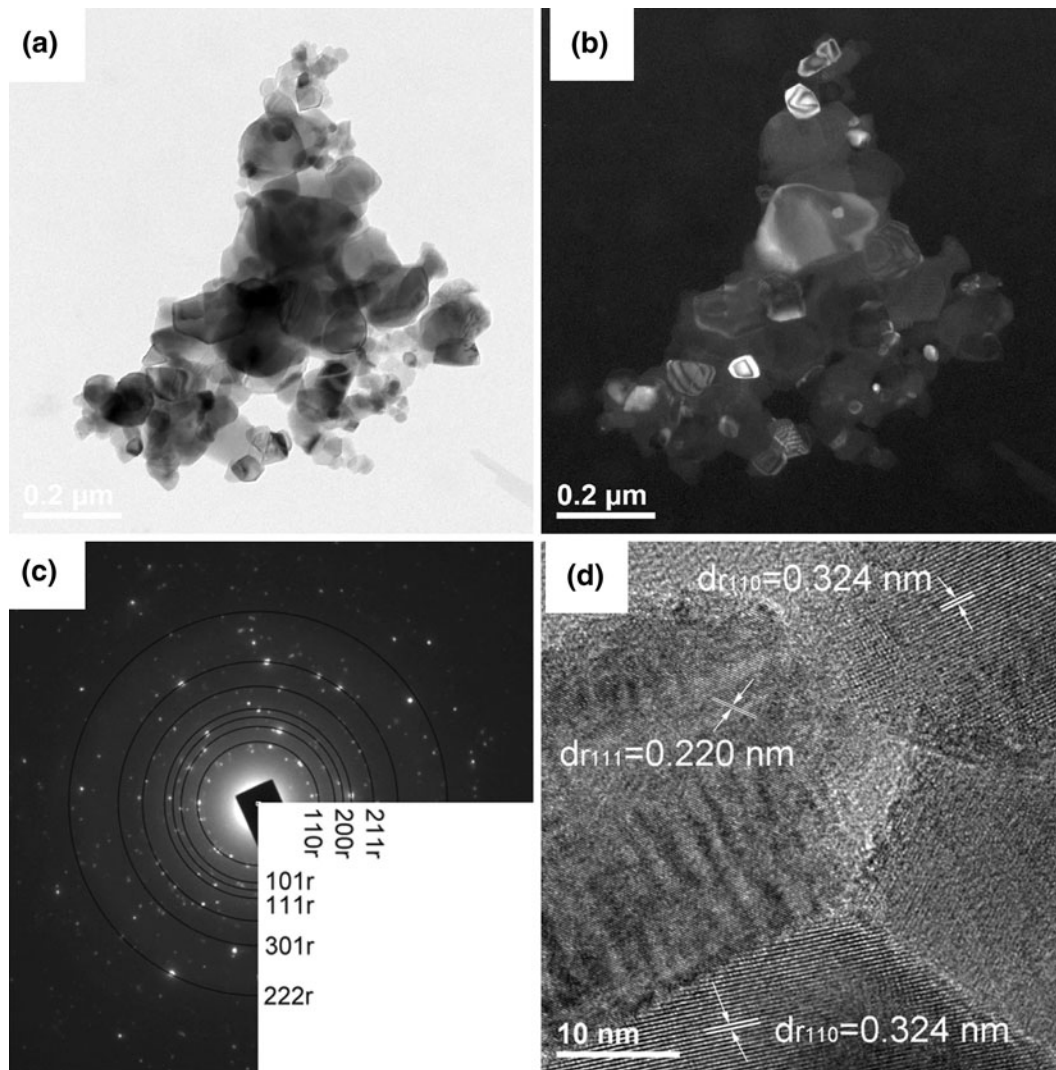

Fig. 8—TEM micrographs of TiO_2 freeze-dried precursor powders after calcination at 973 K (700 °C) for 120 minutes: (*a*) BF image, (*b*) DF image using r-TiO_2 (110) in (*c*), (c) SAED pattern which indexed corresponding to r-TiO_2, (*d*) HRTEM image with *d*-spacing of the r-TiO_2 (110) and (111) were 0.324 and 0.220 nm, respectively.

was reported by Kumar et al.[17,18] These values were smaller than that obtained values in the present study. This result can be suggested to the different initial materials and various prepared processes.

E. *The TEM Microstructure of the TiO$_2$ Freeze-Dried Precursor Powders After Calcination*

The TEM micrographs, SAED pattern, and HRTEM image of the TiO$_2$ freeze-dried precursor powders after calcination at 673 K (400 °C) for 120 minutes were shown in Figure 7. Figure 7(a) shows the bright field (BF) image of the crystallites with a size of about 10 nm, which was consistent with the results shown in Figure 4. Figure 7(b) shows the dark field (DF) image from a-TiO$_2$ (101) reflection in Figure 7(c). Figure 7(c) shows the SAED pattern which indexed corresponding to a-TiO$_2$. Figure 7(d) shows an image of HRTEM with the *d*-spacings of (101) and (111) a-TiO$_2$ of 0.347 and 0.165 nm, respectively.

Figure 8 shows the TEM micrographs, SAED pattern, and HR-TEM image of the TiO$_2$ freeze-dried precursor powders after calcination at 973 K (700 °C) for 120 minutes. Figures 8(a) and (b) shows the BF and DF images, which revealed various crystallite agglomerate and individual crystallite with size of about 37 nm. Figure 8(c) shows the SAED pattern which indexed corresponding to r-TiO$_2$. Figure 8(d) shows the lattice image of HRTEM with the lattice fringe. The lattice fringes indexed corresponding to the *d*-spacings (111) and (110) for r-TiO$_2$ were 0.220 and 0.324 nm, respectively.

IV. CONCLUSIONS

Thermal behavior and phase transformation of TiO$_2$ freeze-dried precursor powders were investigated using DSC/TG, XRD, TEM, and SAED. The results of the present study are summarized as follows:

1. The main compound of TiO$_2$ freeze-dried precursor powders has been determined as TiO$_2$·H$_2$O.
2. XRD results showed that when the TiO$_2$ freeze-dried precursor powders after calcination at 773 K and 873 K (500 °C and 600 °C) for 120 minutes, the crystalline structures were composed of a-TiO$_2$ and r-TiO$_2$ coexist. The a-TiO$_2$ was fully converted to r-TiO$_2$ when the TiO$_2$ freeze-dried precursor powders after calcination at 973 K (700 °C) for 120 minutes.
3. When the TiO$_2$ freeze-dried precursor powders after calcination between 473 K and 873 K (200 °C and 600 °C) for 120 minutes, the crystallite size of a-TiO$_2$ increased from 3.5 to 23.2 nm. Whereas, the crystallite size of r-TiO$_2$ increased from 17.4 to 48.1 nm when calcined from 773 K to 1073 K (500 °C to 800 °C) for 120 minutes.
4. The activation energy of the a-TiO$_2$ formation from the TiO$_2$ freeze-dried precursor powders was 242.4 ± 33.9 kJ/mol, whereas, the activation energy

of phase transformation from a-TiO$_2$ to r-TiO$_2$ was 267.5 ± 19.1 kJ/mol.

REFERENCES

1. C. Gelis, S. Girard, A. Mavon, M. Delverdier, N. Paillous, and P. Vicendo: *Photodermatol. Photoimmunol. Photomed.*, 2003, vol. 19 (5), pp. 242–53.
2. W. Zhang, Y. He, and Q. Qi: *Mater. Chem. Phys.*, 2005, vol. 93, pp. 508–15.
3. G. Dagan and M. Tomkiewicz: *J. Phys. Chem.*, 1993, vol. 97, pp. 12651–55.
4. K. Katayama, H. Hasegawa, T. Noda, T. Akiba, and H. Yanagida: *Sens. Actuators B*, 1990, vol. 2, pp. 143–49.
5. U. Diebold: *Surf. Sci. Rep.*, 2003, vol. 48, pp. 53–229.
6. U. Balachandran and N.G. Eror: *J. Solid State Chem.*, 1982, vol. 42, pp. 276–82.
7. A. Dabler, A. Feltz, J. Jung, W. Ludwig, and E. Kaisersberger: *J. Therm. Anal. Calorim.*, 1988, vol. 33, pp. 803–09.
8. J.G. Li and T. Ishigaki: *Acta Mater.*, 2004, vol. 52, pp. 5143–50.
9. H.K. Park, Y.T. Moon, and D.K. Kim: *J. Am. Ceram. Soc.*, 1996, vol. 79, pp. 2727–32.
10. Y.Q. Zheng, E.R. Shi, Z.Z. Chen, W.J. Li, and X.F. Hu: *J. Mater. Chem.*, 2001, vol. 11, pp. 1547–51.
11. C.H. Lu and M.C. Wen: *J. Alloys. Compd.*, 2008, vol. 448, pp. 153–58.
12. J. Liu, T. An, G. Li, N. Bao, G. Sheng, and J. Fu: *Microporous Mesoporous Mater.*, 2009, vol. 124, pp. 197–203.
13. F. Cot, A. Larbot, G. Nabias, and L. Cot: *J. Eur. Ceram. Soc.*, 1998, vol. 18, pp. 2175–81.
14. J. Yang, S. Mei, and J.M.F. Ferreira: *J. Am. Ceram. Soc.*, 2001, vol. 84, pp. 1696–1702.
15. H.I. Hsiang and S.C. Lin: *Mater. Chem. Phys.*, 2006, vol. 95, pp. 275–79.
16. H.I. Hsiang and S.C. Lin: *Ceram. Int.*, 2008, vol. 34, pp. 557–61.
17. K.N.P. Kumar, K. Keizer, and A.J. Burggraaf: *J. Mater. Chem.*, 1993, vol. 3, pp. 1141–49.
18. K.N.P. Kumar, K. Keizer, A.J. Burggraaf, T. Okubo, and H. Nagamoto: *J. Mater. Chem.*, 1993, vol. 3, pp. 1151–59.
19. Y.W. Hsu, K.H. Yang, K.M. Chang, S.W. Yeh, and M.C. Wang: *J. Alloys Compd.*, 2011, vol. 509, pp. 6864–70.
20. G. Li, L. Li, J. Boerio-Goates, and B.F. Woodfield: *J. Am. Chem. Soc.*, 2005, vol. 127, pp. 8659–66.
21. N. Nakayama and T. Hayashi: *Colloids Surf. A*, 2008, vol. 317, pp. 543–50.
22. M. Henry, J.P. Jolivet, and J. Livage: *Aqueous Chemistry of Metal Cations, Hydrolysis, Condensation, and Complexation*, Springer, Berlin, 1992, p. 155.
23. S.T. Aruna, S. Tirosh, and A. Zaban: *J. Mater. Chem.*, 2000, vol. 10, pp. 2388–91.
24. D. Zhang, L. Qi, J. Ma, and H. Chang: *J. Mater. Chem.*, 2012, vol. 12, 3677–80.
25. H.I. Hsiang and S.C. Lin: *Mater. Sci. Eng. A*, 2004, vol. 380, pp. 67–72.
26. H.S. Liu, T.S. Chin, S.Y. Chiu, K.H. Chung, C.S. Chang, and M.T. Liu: *Ceram. Int*, 1997, vol. 23, pp. 19–25.
27. C.W. Kuo, Y.H. Shen, S.B. Wen, H.E. Lee, I.M. Hung, H.H. Huang, and M.C. Wang: *Ceram. Int.*, 2011, vol. 37, pp. 341–47.

28. R.A. Spurr and H. Myers: *Anal. Chem. Res.*, 1957, vol. 29, pp. 760–62.
29. R.K. Keswani, H. Ghodke, D. Sarkar, K.C. Khilar, and R.S. Srinivasa: *Colloids Surf. A*, 2010, vol. 369, pp. 75–81.
30. C. Marinescu, A. Sofronia, C. Rusti, R. Piticecu, V. Badilita, E. Vasile, R. Baies, and S. Tanasescu: *J. Therm. Anal. Calorim.*, 2011, vol. 103, pp. 49–57.
31. B.D. Cullity: *Elements of X-ray Diffraction*, Addison-Wesley, Reading, MA, 1967, p. 170.
32. A. Marotta and A. Buri: *Thermchim. Acta*, 1978, vol. 25, pp. 155–60.
33. Y.F. Chen, M.C. Wang, and M.H. Hon: *J. Eur. Ceram. Soc.*, 2004, vol. 24, pp. 2389–97.
34. H. Zhang and J.F. Banfield: *Chem. Mater.*, 2002, vol. 14, pp. 4145–54.